The Astrophysical Journal, 954:81 (13pp), 2023 September 1 https://doi.org/10.3847/1538-4357/ace35b

The Crucial Role of Perpendicular Diffusion in the Longitude Distribution of >10 MeV Solar Energetic Protons

Yang Wang[1,2] and Gang Qin[1,2]
[1] School of Science, Harbin Institute of Technology, Shenzhen 518055, People's Republic of China; ywangsz@hit.edu.cn
[2] Shenzhen Key Laboratory of Numerical Prediction for Space Storm, Harbin Institute of Technology, Shenzhen 518055, People's Republic of China
qingang@hit.edu.cn
Received 2023 April 29; revised 2023 June 30; accepted 2023 July 1; published 2023 August 24

Abstract

Gradual solar proton events are thought to consist of solar components originating near the Sun and interplanetary components associated with interplanetary shocks, and the role of interplanetary shocks is considered to be crucial in supplying particles to regions that are not magnetically connected to the solar source region. We calculate the ratios of the peak intensities for the four energy channels (13–16, 20–25, 32–40, and 40–64 MeV) and compare the ratios observed by multiple spacecraft at different locations. We often find that the ratio of peak intensities observed at different locations in the same event remains almost constant as the energy varies. In other words, the ratio of peak intensities from the different energy channels remains almost constant as the position of the spacecraft changes. The phenomenon implies that in many gradual events, energetic particles observed at different locations are mainly composed of solar components that undergo perpendicular diffusion in both the vicinity of the Sun and the interplanetary space, and that perpendicular diffusion is the main factor enabling energetic particles to be observed in regions without magnetic connection to the solar source region.

Unified Astronomy Thesaurus concepts: Solar energetic particles (1491); Interplanetary physics (827); Solar particle emission (1517); Solar storm (1526)

Supporting material: figure set

1. Introduction

Solar energetic particle (SEP) events are composed of solar components from the corona and interplanetary components associated with interplanetary shocks. In general, for energies ranging from a few tens of kiloelectronvolts to a few megaelectronvolt protons, particle intensity variations are often associated with interplanetary shocks. In many events, the temporal variation in particle intensity indicates that the passage of a shock is accompanied by a significant peak, and particle events accelerated by interplanetary shocks are called energetic storm particle (ESP) events (Bryant et al. 1962). However, for >10 MeV proton, there is no significant enhancement in particle intensity as the shock passes the spacecraft in most events. Due to the large spatial scale of interplanetary shocks and the limited number of spacecraft, the absence of ESP events does not mean that interplanetary shocks do not contribute to particle intensity. Therefore, it is not a trivial question as to whether interplanetary shocks play crucial roles in energetic proton events above 10 MeV.

There are three important variables that affect the intensities of energetic particles observed by spacecraft: (1) the heliospheric longitude of the source region, (2) the strength of the interplanetary shock, and (3) the energy of particles. These factors lead to the observation of different intensity–time profiles of energetic particles at different longitude locations. Based on the results of an analysis of energetic proton events observed by the IMPs 4, 5, 7, 8, and ISEE 3 spacecraft in the energy range of 1–300 MeV, Cane et al. (1988) proposed that the intensity–time profiles of solar proton events show that the main controlling factor in the organization of the solar longitude dependence is the presence of interplanetary shocks. For an interplanetary shock, the acceleration is strongest in the center of the shock, i.e., at the nose, and weaker on both sides of the nose. If the observer is facing in the direction of the nose of the shock, the peak time of intensity is close to the moment when the shock passes the observer. If the observer is at the western side of the nose of the shock, the peak of intensity usually appears when the shock is beyond the observer, as the observer is connected to the nose of the shock by magnetic field lines (MFLs). If the observer is at the eastern side of the nose of the shock, the interplanetary shock has little effect on particle intensity, and the peak of intensity appears before the shock passes the observer.

Gradual energetic particle events in interplanetary space are often closely associated with interplanetary shocks. Cane et al. (1988) suggested that interplanetary shocks play a crucial role in providing particles to the regions without magnetic connections to solar source regions. The result leads to a cause-and-effect model that interplanetary shocks are the essential cause of multiple spacecraft at different interplanetary locations observing the same energetic particle event. Interplanetary shocks continuously accelerate particles in the solar wind, and such acceleration continues as the shock propagates to Earth and beyond. This paradigm, referred to in this paper as the *paradigm of interplanetary shock acceleration*, dominates the popular view of the relation between solar activity and energetic particle events (Reames 1999, 2017), and provides much of the practical basis for the study of energetic particles. There have been a number of attempts to calculate the intensity–time profiles in the case of solar particle acceleration by interplanetary shocks (Lee 1983; Gordon et al. 1999; Zank

et al. 2000; Li et al. 2003; Rice et al. 2003; Sokolov et al. 2004; Lee 2005; Verkhoglyadova et al. 2009; Rouillard et al. 2011). Changes in the properties of the shock acceleration as a function of the observer's field line connection to the shock have also been considered theoretically (Heras et al. 1992, 1995; Kallenrode & Wibberenz 1997; Lario et al. 1998; Ng et al. 1999; Kallenrode 2001; Wang et al. 2012; Qin et al. 2013; Qin & Wang 2015). In these papers, intensity–time profiles of energetic protons are interpreted as a consequence of particle acceleration by interplanetary shocks.

The biggest defect of the paradigm of interplanetary shock acceleration is that it is based on the analysis of many events observed from one location (Earth) and cannot explain the relations among particle intensities observed by multiple spacecraft. For example, in studies using observational data from multiple spacecraft, it has been found that the intensities observed by different spacecraft are close to each other during the decay phase, a phenomenon known as a *reservoir* (McKibben 1972; Roelof et al. 1992). McKibben (1972) suggested that interplanetary perpendicular diffusion is responsible for the reservoir phenomenon. Using observational data, some studies have suggested that perpendicular diffusion plays an important role during the decay phase (McKibben et al. 2001a, 2001b; Lario 2010; Wang et al. 2021), leading to the reservoir phenomenon. In numerical simulations, the effect of perpendicular diffusion on the particle intensity at different locations has been investigated and the reservoir phenomenon has been reproduced (Zhang et al. 2009; He et al. 2011; Qin et al. 2013; Qin & Wang 2015). Furthermore, some ^{3}He-rich SEP events show that energetic particles are distributed on a much larger scale than the source region. The origin of ^{3}He-rich SEP events is generally believed to be related to the acceleration process of flares. Wiedenbeck et al. (2013) reported ^{3}He-rich SEP events that occurred between 2007 January and 2011 January, and extensively studied an event that occurred on 2010 February 7, using data from the ACE and the two STEREO spacecraft. Interestingly, all three spacecraft detected the 2010 February 7 event, with a range of 136° in longitude. They discussed several possible mechanisms that could cause flare-accelerated particles to be distributed across a wide range of longitudes, including interplanetary perpendicular diffusion.

The pitch angle distribution of energetic particles is also important information that reflects the diffusion process of particles. For energetic protons, Zhang et al. (2009) used numerical simulations to investigate the particle anisotropy and found significant anisotropy only in situations with direct magnetic connections. They proposed that anisotropy could be a powerful test for direct magnetic connections with solar particle sources. For energetic electrons, Dresing et al. (2012) studied an SEP event observed by two STEREO spacecraft and SOHO on 2010 January 17. The longitudinal diffusion of energetic particles in this event was close to 360° at 1 AU. The characteristic of this event was that the starting time of energetic particles has a strong delay compared with flares, and there was little or no anisotropy in the intensity measurements at all three locations. By comparing numerical results with observational results, they suggested that perpendicular diffusion in interplanetary space could explain the observational results. Dresing et al. (2014) utilized two STEREO and a near-Earth spacecraft (SOHO or ACE) to study a set of SEP events seen by at least two spacecraft from 2009 to mid-2013. They paid special attention to the anisotropy of energetic electrons to distinguish the sources and transport mechanisms in the widespread events. They suggested that the extended solar source region and the perpendicular diffusion in the interplanetary space are two important mechanisms that cause widespread events. Furthermore, using numerical simulations, Strauss et al. (2017) suggested that the effects of perpendicular diffusion could explain the wide range of longitudinal propagation of energetic electrons.

In gradual energetic proton events, both interplanetary shock acceleration and perpendicular diffusion effects are possible in providing particles to regions not magnetically connected to solar sources. It remains to be investigated whether the causes of gradual events observed simultaneously by widely separated spacecraft are acceleration of interplanetary shocks or effects of perpendicular diffusion, or whether both play important roles. In this paper, we study the intensity–time profiles of 13–64 MeV proton using three spacecraft STEREO A, STEREO B, and SOHO near 1 AU in the ecliptic. In Section 2, we investigate the ratios of peak intensities in different energy channels of the proton events observed by the three spacecraft and present statistics of the peak intensity ratios in different SEP events. In Section 3, we discuss the transport mechanisms of energetic protons. Finally, Section 4 summarizes the results of this work.

2. Energetic Proton Events Observed by Multiple Spacecraft

Data from three spacecraft STEREO A, STEREO B, and SOHO located at ecliptic 1 AU were used in this work. STEREO A and STEREO B were launched 2006 October 25, moving away from each other with an angular velocity of 44° per year, and SOHO was always around the first Lagrangian point. Energetic proton data from SOHO are measured by the High Energy and Relativistic Nucleon and Electron instrument, and the near-Earth solar wind data are provided by OMNIWeb. The solar wind and energetic energy proton data from STEREO A and B were measured by the plasma and superthermal ion components and the in situ measurements of particle and CME transients. The energy channels of energetic protons for SOHO are 13–16, 20–25, 32–40, and 40–64 MeV, while energy channels for STEREO A and STEREO B are 13.6–15.1, 20.8–23.8, 33.4–40.5, and 40–60 MeV, respectively. In the following, the four energy channels of protons are labeled as 13–16, 20–25, 32–40 , and 40–64 MeV, respectively. In this paper, the unit of intensity is $(\mathrm{cm}^2 \cdot \mathrm{sr} \cdot \mathrm{s} \cdot \mathrm{MeV})^{-1}$.

Comparing data from STEREO A, STEREO B, and SOHO spacecraft for >10 MeV proton events, we find that the higher the peak intensity of energetic particles is, the earlier the peak tends to arrive. Therefore, we can define the spacecraft that observes the earliest peak time and the highest peak intensity as the highest peak intensity spacecraft in every energetic proton event, abbreviated as HPI spacecraft, which is the same for all energy channels. In a previous study (Wang et al. 2022), we statistically studied the peak times of STEREO A, STEREO B, and SOHO spacecraft for 13–64 MeV energetic proton events from 2010–2014. In Figure 1, by the end of 2010, the longitudinal difference between STEREO A and STEREO B exceeded 130°. The symmetrical distribution of the three spacecraft provides good monitoring of the particle intensity distribution at different longitudes in the ecliptic near 1 AU.

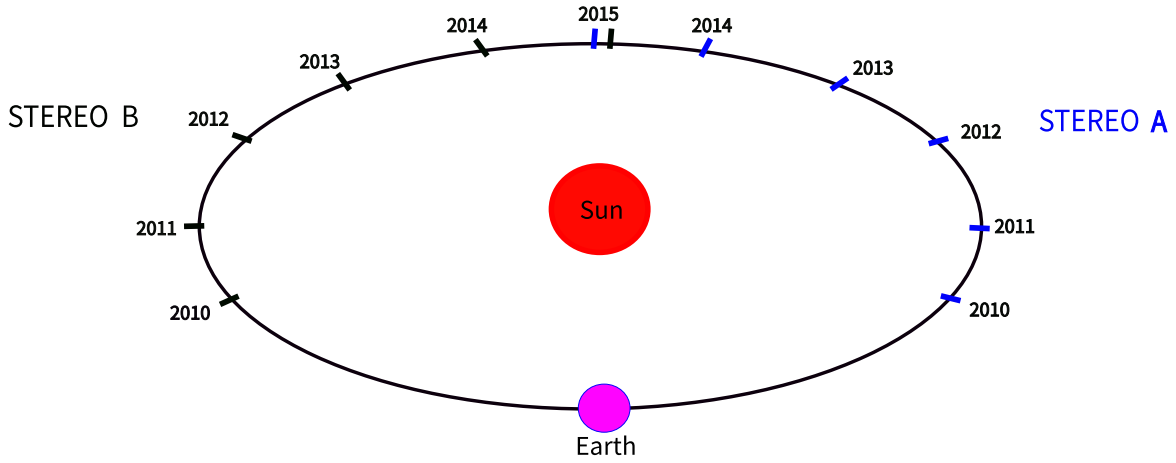

Figure 1. Locations of the Earth (SOHO) and the two STEREO spacecraft in the ecliptic plane between 2010 January and 2015 June.

Our statistical study shows that in the cases without ESP event or multiple peaks, the peak times of intensities for >10 MeV energetic protons observed by the HPI spacecraft are often only a few hours to a dozen hours, or at most a day, after solar eruptions. For 13–16, 20–25, 32–40, and 40–64 MeV energetic proton events, the average peak times are 9.12, 7.56, 6.40, and 5.55 hr, respectively, and the median of peak times are 7.36, 6.02, 5.08, and 3.93 hr, respectively. In this case, for >10 MeV protons, the acceleration of these particles observed by the HPI spacecraft in most cases occurs in the vicinity of the Sun. These particles are produced by flares or coronal shocks, and are not related to the acceleration of interplanetary shocks since in such a short time range, shocks are still not far away from the Sun.

2.1. Two Typical Gradual Energetic Proton Events without ESPs

Figure 2 shows intensity–time profiles of energetic protons observed by STEREO A, STEREO B, and SOHO on 2013 October 11. Among the particle intensities observed by the three spacecraft, and STEREO A, which observed the fastest increase in intensity during the rising phase, is the HPI spacecraft in the event. For 13–16 , 20–25, 32–40, and 40–64 MeV energetic protons, the peak times observed by STEREO A are about 4.36, 3.45, 2.86, and 2.56 hr after solar eruption, respectively. A rapid increase in intensity was also observed by STEREO B, while a slow increase in intensity was observed by SOHO, with a rising process approaching 4 days. The slow increase in the intensity of the SOHO observation is due to the fact that the magnetic footpoint of SOHO is far from the solar source region, so particles do not follow the MFLs from the solar source region to the SOHO spacecraft. STEREO A observed the largest peak intensity and SOHO observed the smallest peak intensity, with a difference of several orders of magnitude. During the energetic proton event, none of the three spacecraft observed an ESP event. The reservoir effect was quite significant after 2013 October 15, when particle intensities observed by the three spacecraft reached uniformity lasting for about 8 days.

In many proton events, fluctuations often occur near the peak of the intensity–time profiles, resulting that the peak intensities cannot be accurately determined merely from the maximum point. Therefore, we approximately estimate peak values from intensity observations. From the time profiles of 13–16 MeV proton intensities, we get the peak values for different spacecraft and determine which is the HPI spacecraft, and additionally, we can get the ratios of peaks between different spacecraft. Here, we denote the ratios as $R_{13-16\mathrm{MeV}}$. In the top panel of Figure 2, the blue, black, and pink horizontal dashed lines indicate peak values for STEREO A, STEREO B, and SOHO, respectively. In the higher energy channels, we can get the peak values from intensity profiles for the HPI spacecraft, and the peak values for other spacecraft by calculating with the ratios $R_{13-16\mathrm{MeV}}$. We can compare the observed particle intensities with the calculated peak values. In panels (b)–(d), the blue horizontal dashed lines indicate the peak value for STEREO A from observations, and the black, and pink horizontal dashed lines indicate peak values for STEREO B and SOHO, respectively, from calculations using the ratio $R_{13-16\mathrm{MeV}}$. It can be seen that the calculated peak values represented by black and pink dashed lines in panels (b)–(d) are close to the peaks of the intensities observed by the three spacecraft. The result indicates that the ratios of peak intensities observed by the three spacecraft remain almost constant as the energy varies. We have $P^{\mathrm{STA}}_{13-16\mathrm{MeV}}$: $P^{\mathrm{STB}}_{13-16\mathrm{MeV}} \approx P^{\mathrm{STA}}_{20-25\mathrm{MeV}}$: $P^{\mathrm{STB}}_{20-25\mathrm{MeV}}$ and $P^{\mathrm{STA}}_{13-16\mathrm{MeV}}$: $P^{\mathrm{SOHO}}_{13-16\mathrm{MeV}} \approx P^{\mathrm{STA}}_{20-25\mathrm{MeV}} : P^{\mathrm{SOHO}}_{20-25\mathrm{MeV}}$. Here, P indicates the peak intensities with superscript and subscript denoting the spacecraft and energy channel, respectively. Then, we can get $P^{\mathrm{STA}}_{13-16\mathrm{MeV}} : P^{\mathrm{STA}}_{20-25\mathrm{MeV}} \approx P^{\mathrm{STB}}_{13-16\mathrm{MeV}} : P^{\mathrm{STB}}_{20-25\mathrm{MeV}} \approx P^{\mathrm{SOHO}}_{13-16\mathrm{MeV}} : P^{\mathrm{SOHO}}_{20-25\mathrm{MeV}}$. Therefore, the ratio of peak intensities from the different energy channels remains almost constant as the position of the spacecraft changes. We call the relations *equal ratio relations*. According to the equal ratio relations, we infer that the particles observed by STEREO B and SOHO have the same origin as the particles observed by STEREO A, originating from the same acceleration process. Since the peak intensity observed by STEREO A was reached very quickly, most of the particles observed by STEREO A originated from the acceleration of flare or shock near the Sun, and are not related to the acceleration of any interplanetary shock. If the particles observed by STEREO B or SOHO originated from the acceleration of an interplanetary shock, the peak intensities observed by the three spacecraft should not satisfy the equal ratio relations. Therefore, based on the equal ratio relations and the reservoir phenomenon, we suggest that the particles reached the MFLs of STEREO B and SOHO by the effects of perpendicular diffusion, and these particles did not originate from the continuous acceleration of any interplanetary shock.

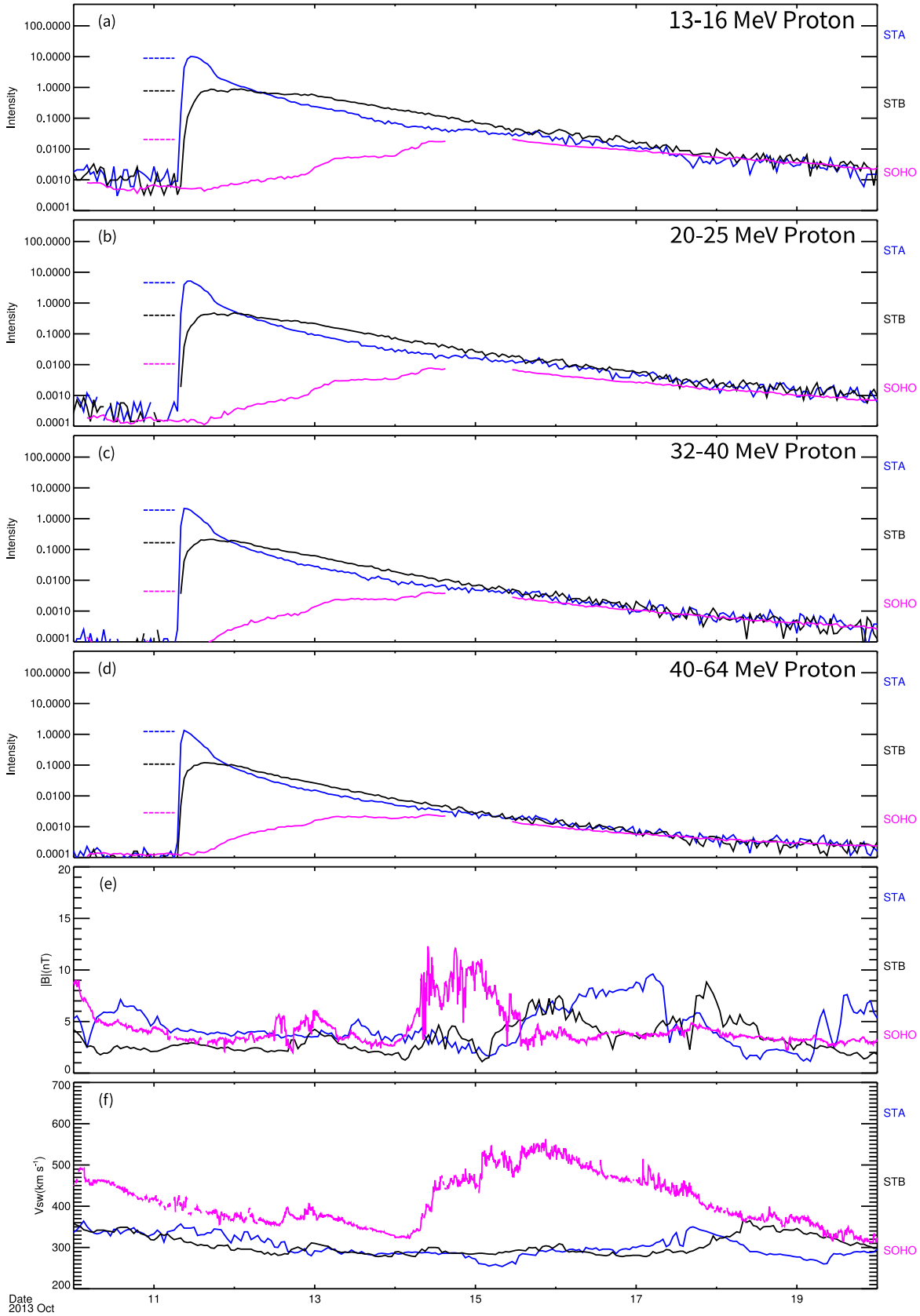

Figure 2. From top to bottom: the energetic proton intensities (panels 1–4), magnetic field intensity (panel 5), and solar wind speed (panel 6) in OMNI data are used instead of the plasma data observed by SOHO to improve the statistics. The horizontal dashed lines represent the peak intensities of the reference, which have the same ratios in each panel.

A possible explanation for the formation of gradual energetic proton events satisfying equal ratio relations is that the events are mainly composed of solar components and perpendicular diffusion is the main factor enabling the gradual events to be observed in regions with no magnetic connection to the solar source region. Particles can transport with parallel and perpendicular diffusion, which can occur both near the Sun and in interplanetary space. In the beginning, perpendicular diffusion occurred near the Sun when energetic particles were released (Zhang & Zhao 2017). Perpendicular diffusion also occurred in interplanetary space, as particles traveled outward away from the Sun. Since interplanetary MFLs are divergent and the strength of the magnetic turbulence decays rapidly with increasing radial distance, particles near the Sun can transport from the source's MFL to another MFL easier than that in the interplanetary space to the same MFL. Therefore, perpendicular diffusion occurring near the Sun may cause the particle intensities observed by STEREO B to increase quickly during the rising phase. However, since the footpoint of SOHO's MFL was far from the solar source, perpendicular diffusion is difficult to make particles reach SOHO's MFL near the Sun. Instead, energetic particles reached SOHO's MFL with perpendicular diffusion after propagating into interplanetary space, so SOHO observed a much slower rise in intensity compared to STEREO A and STEREO B. During the rising phase, there was a huge difference in particle intensity at different locations depending on the magnetic connectivity to the solar source. Due to perpendicular diffusion, the intensities of particles at different locations gradually became uniform over time, and the spatial gradients of intensities decreased with time. In the decay phase, the intensity of energetic particles observed by SOHO gradually became the same as that observed by STEREO A and B, and the reservoir phenomenon appeared.

Figure 3 shows an energetic proton event observed by STEREO A, STEREO B, and SOHO on 2011 November 3, with the same format as that in Figure 2. In the event, STEREO A is the HPI spacecraft. For 13–16, 20–25, 32–40, and 40–64 MeV protons observed by STEREO A, peak times of intensities were 6.23, 4.66, 3.05, and 2.38 hr, respectively. During this event, the increases in intensities observed by all three spacecraft were rapid, and the peak times observed by all three spacecraft were almost the same, since energetic particles underwent perpendicular diffusion in the vicinity of the Sun at the beginning. As time passed, particles traveled outward along MFLs with perpendicular diffusion in interplanetary space. Therefore, STEREO A, STEREO B, and SOHO observed the reservoir phenomenon 2 days later, showing similar intensities during the decay phase of the particle intensity.

In the 2011 November 3 event, the peaks of intensities observed by STEREO B and SOHO were nearly the same. In this case, we use only one dashed line instead of two to indicate the peaks observed by STEREO B and SOHO. The ratio of peak particle intensities observed by the three spacecraft are close in the four different energy channels. In other words, the ratio of peak intensities from the different energy channels remains almost constant as the position of the spacecraft changes. According to the equal ratio relations, we infer that the particles observed by STEREO B and SOHO come from the same acceleration process as the particles observed by STEREO A. Therefore, based on the equal ratio relations and the reservoir phenomenon, we suggest that the particles observed by STEREO B and SOHO come from perpendicular diffusion, rather than the continuous acceleration of an interplanetary shock.

2.2. A Typical Gradual Energetic Proton Event with ESPs

Figure 4 shows an energetic proton event observed by STEREO A, STEREO B, and SOHO on 05 March 2013, with the same format as that in Figure 2. In the event, STEREO A is the HPI spacecraft. For 13–16 MeV protons, STEREO B observed an interplanetary shock driven by an interplanetary coronal mass ejection (ICME), accompanied by an increase in energetic particles forming an ESP event. The interplanetary shock passed STEREO B at 12:23 pm on March 7 (Kilpua et al. 2015), while the magnetic obstacle of the ICME passed through STEREO B between 8:00 pm on March 8 and 8:45 pm on March 10 (Jian et al. 2018). When the shock passed STEREO B, the intensity of 13–16 MeV proton observed by STEREO B exceeded that observed by STEREO A. After the shock passage of STEREO B, the particle intensities observed by STEREO B decayed quickly. Because the acceleration efficiency of interplanetary shock decreases with the energy of protons, the 13–16 MeV protons observed by STEREO B during the peak were accelerated efficiently by the ICME shock, but the 40–64 MeV protons observed by STEREO B during the peak were only accelerated efficiently near the Sun. Therefore, the peak time of the intensity of 13–16 MeV protons observed by STEREO B was more than 1 day later than that of the 40–64 MeV protons.

In this event, particle intensities observed by STEREO A and SOHO satisfy the equal ratio relations, but particle intensities observed by STEREO B do not satisfy the equal ratio relations with that observed by STEREO A or SOHO. It can be seen that in panels (b)–(d), the ratio of the peaks was not the same as that in panel (a). The main reason was the existence of two different components of particles observed by STEREO B, a solar component originating near the Sun and an interplanetary component associated with interplanetary shock. For 13–16 MeV protons, the interplanetary component dominates the peak of intensity observed by STEREO B. For 40–64 MeV protons, on the other hand, the solar component dominates the peak of the intensity observed in STEREO B. Since the two components are not the same, there are no equal ratio relations between the intensity of particles observed by STEREO B and that observed by STEREO A or SOHO. Due to the effects of perpendicular diffusion, the intensity of particles observed by STEREO A and SOHO was also affected by the acceleration of interplanetary shock. In this event, for STEREO A and SOHO observations, however, since the acceleration of interplanetary shock was limited, energetic particles were dominated by the solar component instead of the interplanetary component, and the peak time of particle intensity was much earlier than the time when the shock passed 1 AU. Therefore, the particle intensities observed by STEREO A and SOHO approximately satisfied the equal ratio relations. If the acceleration of the shock was stronger in this event, there might be no equal ratio relations between the particle intensities observed by STEREO A and SOHO.

2.3. Statistical Results of Energetic Particle Events

We have studied statistically the peak ratios of particle intensities observed by at least two spacecraft at different

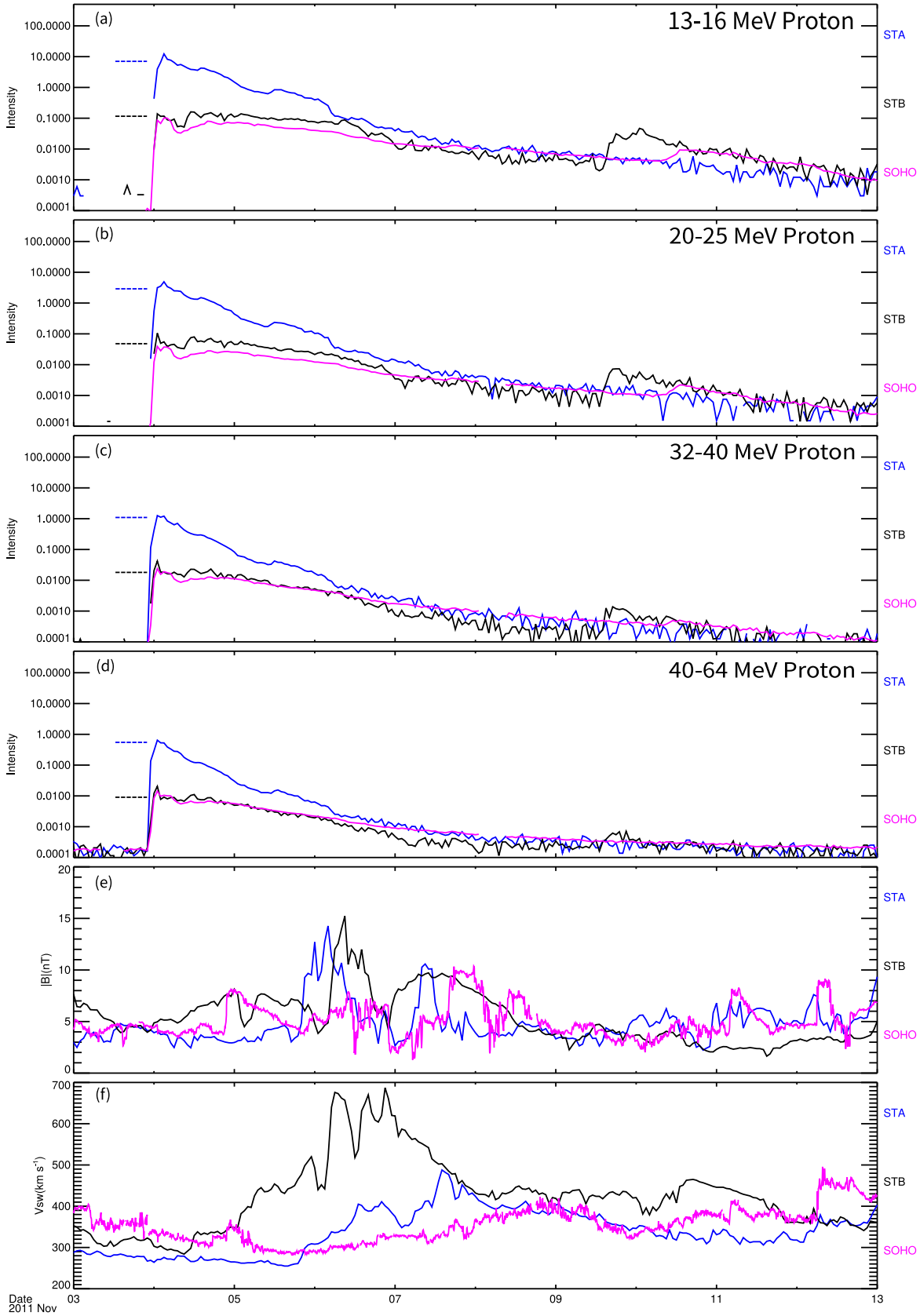

Figure 3. As in Figure 2 for the 2011 November 3 event. The peaks observed by STEREO B and SOHO are so close that only one dashed line, rather than two, is used to represent the peaks observed by STEREO B and SOHO.

locations. Beginning in 2007–2014 September (before STEREO B was lost), we found that the peak ratios of intensities observed by different spacecraft were approximately equal in 55 events. Because the solar activity was weak before 2010, all of the events occurred between 2010 and 2014. In Table 1, we list all the events that satisfy the equal ratio

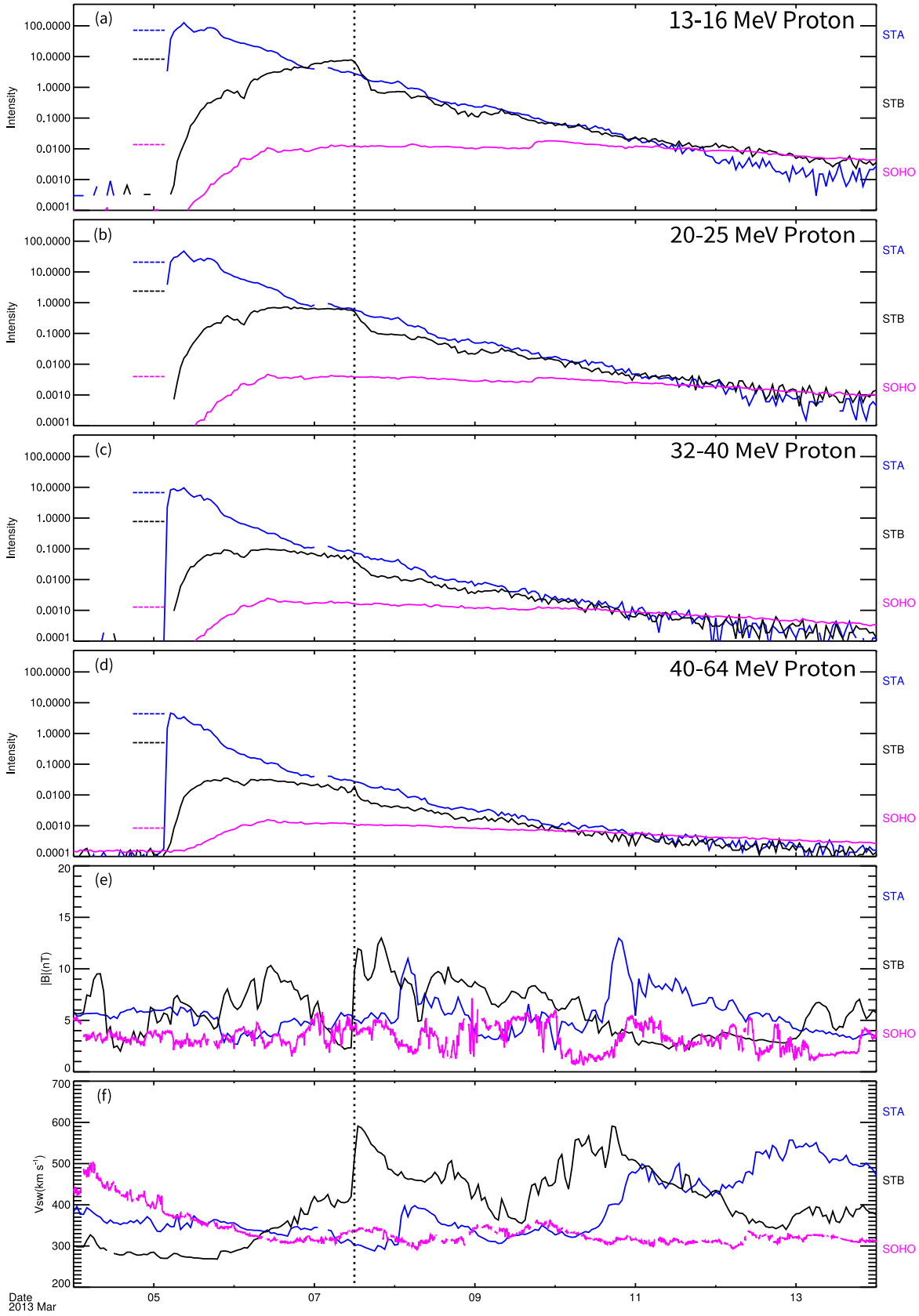

Figure 4. As in Figure 2 for the 2013 March 5 event. The vertical dotted line indicates the moment when the shock passed STEREO B near 1 AU.

relations and calculate the reference ratios of the peaks of intensities in each event, with the information on solar events in the SEP events mainly provided by Richardson et al. (2014) and Paassilta et al. (2018). All the events and the reference ratios of the peak intensities in Table 1 are shown in Figure 5.

Table 1
Energetic Proton Events That Satisfy the Equal Ratio Relations Observed by STEREO-A, STEREO B, and SOHO

No.	Solar Event (UT) YYYY-MM-DD HH	Flare Earth (°)	Spacecraft	I1/I2	I1/I3
1	2010-08-01 07	E36	B, S	2.01E+02	
2	2010-08-07 17	E34	B, S	2.18E+01	
3	2010-08-14 09	W54	S, B, A	2.29E+01	3.10E+02
4	2010-08-18 05	W100	S, A, B	1.00E+00	1.44E+01
5	2010-08-31 21	W145	A, S	3.11E+00	
6	2010-09-08 23	W92	A, S, B	1.00E+00	9.54E+00
7	2011-01-28 00	W90	S, A	3.45E+00	
8	2011-02-15 01	W18	B, S	5.53E+00	
9	2011-03-07 19	W53	B, S	1.00E+00	
10	2011-03-21 02	W138	A, S	1.04E+02	
11	2011-08-04 03	W36	S, B, A	2.11E+02	2.11E+02
12	2011-09-22 10	E78	B, A	1.00E+00	
13	2011-10-04 12	E148	B, A, S	5.48E+00	1.84E+02
14	2011-11-03 22	E152	A, B, S	6.17E+01	6.17E+01
15	2011-11-17 22	E125	B, A, S	3.74E+01	3.74E+01
16	2012-01-19 13	E30	B, S	1.07E+01	
17	2012-01-23 04	W21	B, A	1.00E+00	
18	2012-03-24 00	E169	A, B	3.54E+01	
19	2012-05-17 01	W76	S, B	6.00E+02	
20	2012-07-08 16	W74	S, A	1.00E+00	
21	2012-07-12 15	E06	S, B	1.00E+00	
22	2012-09-08 11	W145	S, A	3.24E+00	
23	2012-09-27 23	W34	B, S	1.00E+00	
24	2012-10-14 00	E138	A, B, S	2.04E+01	1.60E+02
25	2012-11-08 11	W168	A, S, B	2.02E+01	1.18E+02
26	2013-03-05 03	E141	A, S	4.92E+03	
27	2013-04-11 06	E12	B, S, A	3.82E+00	4.10E+03
28	2013-04-21 06	W124	S, A	1.33E+01	
29	2013-04-24 21	W175	A, S	5.80E+00	
30	2013-05-01 02	E105	A, B	1.00E+00	
31	2013-05-22 12	W70	S, B	4.15E+02	
32	2013-06-21 02	E73	B, S, A	8.53E+00	4.11E+02
33	2013-07-01 20	E90	B, A	7.73E+00	
34	2013-07-22 06	W172	A, B	4.19E+01	
35	2013-08-30 02	E43	B, S	1.03E+02	
36	2013-10-05 08	E123	A, B	2.80E+01	
37	2013-10-11 07	E96	A, B, S	1.13E+01	4.46E+02
38	2013-10-22 21	0	S, B	5.08E+00	
39	2013-10-25 08	E73	B, S	6.85E+01	
40	2013-11-02 04	W127	A, B	3.68E+01	
41	2013-12-26 03	E161	A, B, S	1.00E+00	3.66E+01
42	2013-12-28 17	W130	S, B, A	1.19E+01	1.19E+01
43	2014-02-09 15	E103	A, B	1.42E+01	
44	2014-02-21 22	E88	B, A	1.58E+01	
45	2014-02-25 00	E82	A, B, S	1.00E+00	1.57E+01
46	2014-03-05 13	E179	A, B	1.57E+01	
47	2014-03-12 14	E158	A, B	1.34E+01	
48	2014-04-02 13	E62	B, A	1.72E+03	
49	2014-05-15 ?	?	A, B	1.10E+01	
50	2014-06-06 13	E132	A, B	2.19E+00	
51	2014-06-10 12	E82	B, A	6.23E+00	
52	2014-07-08 16	E56	B, S	7.91E+00	
53	2014-08-28 ?	?	A, B	8.90E+01	
54	2014-09-01 11	E127	B, S	6.92E+02	
55	2014-09-10 17	E02	S, B	1.28E+01	

Note. Column 1: the ordinal number of the solar event. Column 2: date and hour of the solar flare. Column 3: longitude of the solar event relative to Earth/SOHO, where E(W) indicates that the flare is east (west) of the spacecraft. Column 4: the spacecraft satisfying the equal ratio relations ordered by their peaks. Column 5: maximum peak intensity (I1) divided by second peak intensity (I2). Column 6: maximum peak intensity divided by third peak intensity (I3) (if there are three spacecraft satisfying the equal ratio relations). A, B, and S are short for STEREO A, STEREO B, and SOHO. The "?" mark means that the solar source of the energetic event has not been identified.

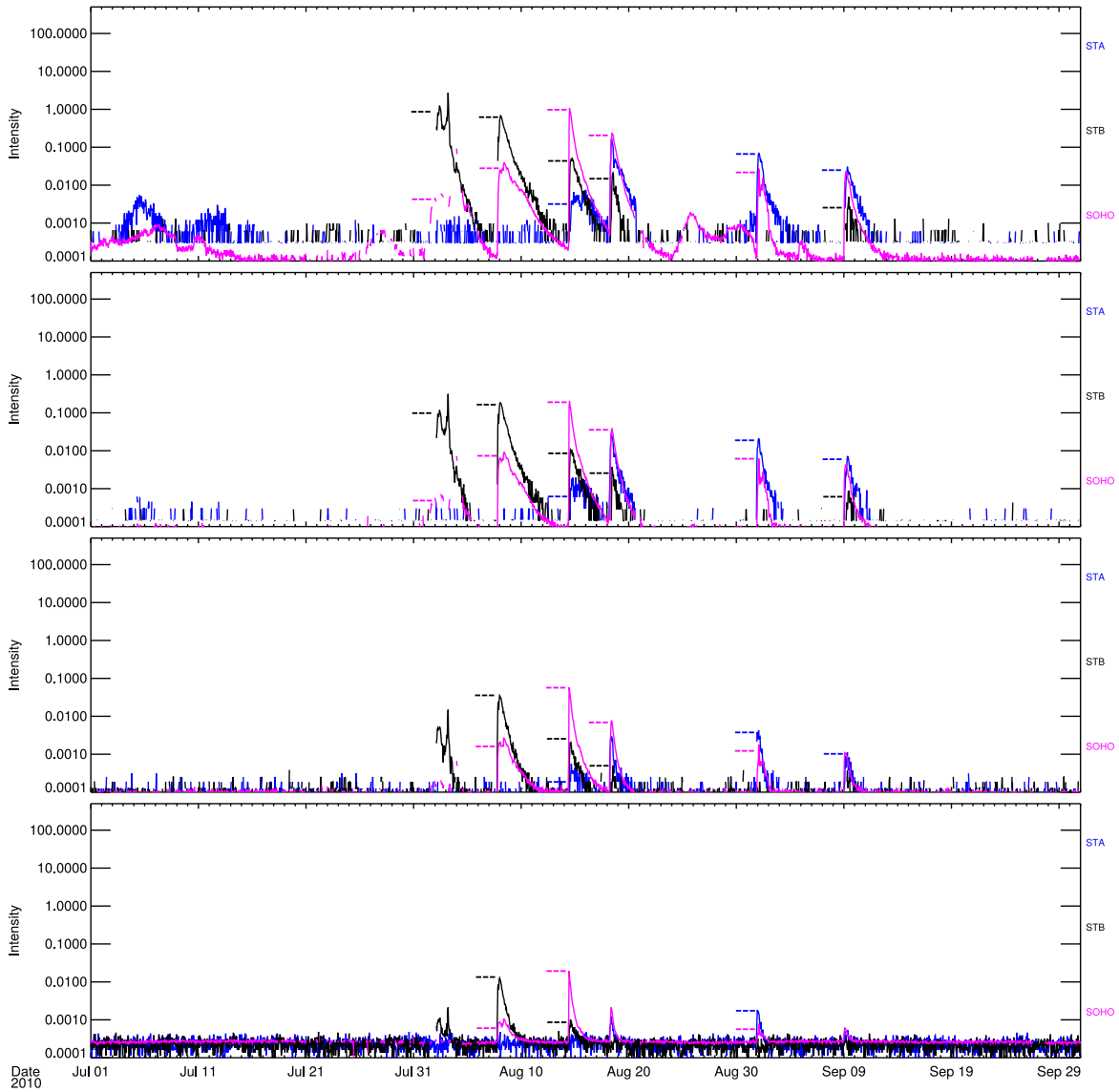

Figure 5. Panels (1)–(4) indicate the intensities of 13–16, 20–25, 32–40, and 40–64 MeV energetic protons during the third quarter of 2010, respectively. The horizontal dashed lines represent the peak intensities of the reference, which have the same ratios in each panel.

(The complete figure set (15 images) is available.)

In Figure 5, we plot the intensity–time profiles of energetic particles for four quarters every year. The four quarters are as follows: January, February, and March (Q1), April, May, and June (Q2), July, August, and September (Q3), and October, November, and December (Q4). During Q1, Q2, and Q4 in 2010, there are no energetic particle events observed by more than one spacecraft. During Q2 of 2011, there is only one multi-peak energetic particle event observed by at least two spacecraft. However, in a multi-peak energetic particle event, the equal ratio relations are not satisfied. Therefore, the four periods of SEP intensity were not plotted. According to Table 1, we give the reference values of the peak intensity represented by the dashed lines in different energy channels.

In the events shown in Figure 5, the reference values represented by dashed lines are so close to the peak intensities that the difference between the reference value and the peak intensity can be easily assessed by eye. In most cases, the dashed lines are drawn to the left of the peaks of intensity. In a few cases, the dashed lines are drawn above the peaks of intensity in order not to block the data observed by the spacecraft. We can find that many single-peak events in which the intensity peaks observed by different spacecraft satisfied the equal ratio relations. In some single-peak events, the peak intensity was so small that it was close to the background intensity, so it is impossible to determine whether equal ratio relations are met. In addition, if the duration of the SEP event is too short, there may not be enough time to reach the perpendicular diffusion limit. Laitinen et al. (2017) used full-orbit particle simulations to analyze the cross-field propagation of 1–100 MeV protons in turbulent magnetic fields. They found that early particle transport follows meandering turbulent MFLs, and is mainly non-diffusive. Laitinen & Dalla (2017) suggested that this pre-diffusion is a significant process for energetic protons. The typical duration of the pre-diffusion phase ranges from several to tens of hours for 10 MeV protons under solar wind turbulence conditions at 1 AU. Therefore, if

the duration of energetic particle events is short, interplanetary cross-field diffusion may not have enough time to occur. In many multi-peak events, the intensity peaks observed by different spacecraft did not satisfy the equal ratio relations for the following reasons. Multi-peak energetic particle events were either generated by the acceleration of interplanetary shocks or by multiple injections from solar source regions, as a result, particles of different origins are mixed together and are not related to each other.

Perpendicular diffusion not only includes cross-field diffusion but also the lateral transport brought about by the random walk of the turbulent MFLs. If the interplanetary scattering is weak, we suggest that the peak energy spectrum of >10 MeV protons observed by well-connected spacecraft may be similar to the injection energy spectrum of the solar source region in the single-peak events. This result is similar to the idea proposed by Strauss et al. (2020). They proposed that for lower energy of energetic electrons, in situations where spacecraft are located close to the Sun, the scattering effects of pitch angle are small. As a result, the energy spectrum of electrons observed by the spacecraft is similar to the injection energy spectrum of energetic electrons in the solar source region. It is worth noting that in interplanetary space, not only the longitudinal perpendicular transport occurs, but also the latitudinal perpendicular transport (Lario 2010; Qin et al. 2013). The perpendicular diffusion coefficients may vary considerably at different locations in the interplanetary space. For instance, Strauss et al. (2016) proposed that perpendicular diffusion is strongly damped at magnetic discontinuities in the presence of shocks. Furthermore, Dalla et al. (2013) proposed that drift may be an important mechanism for the transport of energetic particles across magnetic fields. Wijsen et al. (2020) analyzed simulated results under magnetic fields of corotating interaction region and found that drifts could be enhanced when the solar wind contains compression region or shock waves, and there is an interplay between drifts and the perpendicular diffusion coefficients (van den Berg et al. 2021). The effects of drift and perpendicular diffusion during the propagation process could be further investigated in the future.

3. Discussion

In the paradigm of Cane et al. (1988), the intensity–time profiles of 1–300 MeV proton intensity depend on the longitudes of the solar events relative to the observer and are primarily related to the presence and strength of interplanetary shocks. In particular, for spacecraft not magnetically connected to the solar sources, the acceleration capability of the interplanetary shocks determines whether energetic particle events could be observed. In this work, we have found the following. In the absence of interplanetary shock acceleration, the perpendicular diffusion process determines whether energetic particle events would be observed by the spacecraft magnetically disconnected from the solar source. However, in the presence of interplanetary shock acceleration, for a spacecraft magnetically disconnected from the solar source, both perpendicular diffusion and the acceleration of the interplanetary shock can affect the intensity of the energetic particle event. Since the shock acceleration region with high efficiency is usually narrow relative to the observed longitudinal distribution range of energetic particles, we suggest that it is the effects of perpendicular diffusion, rather than interplanetary shocks, that play a key role in the longitudinal distribution of most >10 MeV gradual solar energetic protons.

In order to study the intensity–time profiles and the propagation processes, a cartoon diagram in Figure 6 has been drawn to show the profiles of the energetic particle events observed at the different locations. Spacecraft A, B, and C are near 1 AU in the ecliptic and the solid black lines denote the MFLs. The dotted lines represent the MFLs connected to the strongest part of the solar source region. The inner and outer dashed–dotted lines represent the perpendicular diffusion of particles near the Sun and perpendicular diffusion in interplanetary space, respectively. The perpendicular diffusion near the Sun is during the early stages, while the perpendicular diffusion in interplanetary space is during the late stages. The directions of the arrows represent the propagation of particles from the solar source region to other longitudes due to perpendicular diffusion.

In panel (a), no acceleration by interplanetary shock is shown, and the energetic particles observed by the three spacecraft A, B, and C are mainly produced by the acceleration of particles near the Sun. The interplanetary magnetic field is assumed to be the Parker model, with the Sun at the center. In this case, the peak intensities observed by the three spacecraft satisfy the equal ratio relations. For the three different spacecraft, we can expect the following scenario.

*Spacecraft A.*The footpoint of spacecraft A's MFL is close to the region of the strongest acceleration, and particles are mainly produced by the acceleration of particles near the Sun. As a result, the particle intensity increases rapidly with time. Among the three spacecraft, the peak intensity of particles observed by spacecraft A is the largest, so spacecraft A is the HPI spacecraft.

Spacecraft B. Energetic particles undergo perpendicular diffusion in the vicinity of the Sun, and particles quickly reach the MFL of spacecraft B. As a result, the particle intensity observed by spacecraft B increases rapidly with time, and the peak intensity of particles observed by spacecraft B is smaller than that observed by spacecraft A.

*Spacecraft C.*The magnetic footpoint of spacecraft C is far from the solar source region. Only a small number of particles can reach the MFL of spacecraft C by perpendicular diffusion in the vicinity of the Sun. The majority of particles reach the MFL of spacecraft C by perpendicular diffusion in interplanetary space. The particle intensity observed by spacecraft C increases slowly with time, with the smallest peak among the peak intensities observed by the three spacecraft.

In panel (b), the interplanetary shock shows a significant acceleration of particles. The ICME and the interplanetary shock driven by ICME are plotted in the panel. The particles observed by the three spacecraft A, B, and C have two different components, which are the solar component originating from the solar corona and the interplanetary component associated with interplanetary shock. In this case, peak intensities observed by the three spacecraft do not satisfy the equal ratio relations. For the three different spacecraft, we have the following scenario.

Spacecraft A. Particles accelerated by interplanetary shock can reach spacecraft A's magnetic field line by perpendicular diffusion. However, due to the dominance of the solar component of spacecraft A, the number of interplanetary shock-accelerated particles reaching spacecraft A is relatively small. Therefore, the interplanetary shock acceleration does not

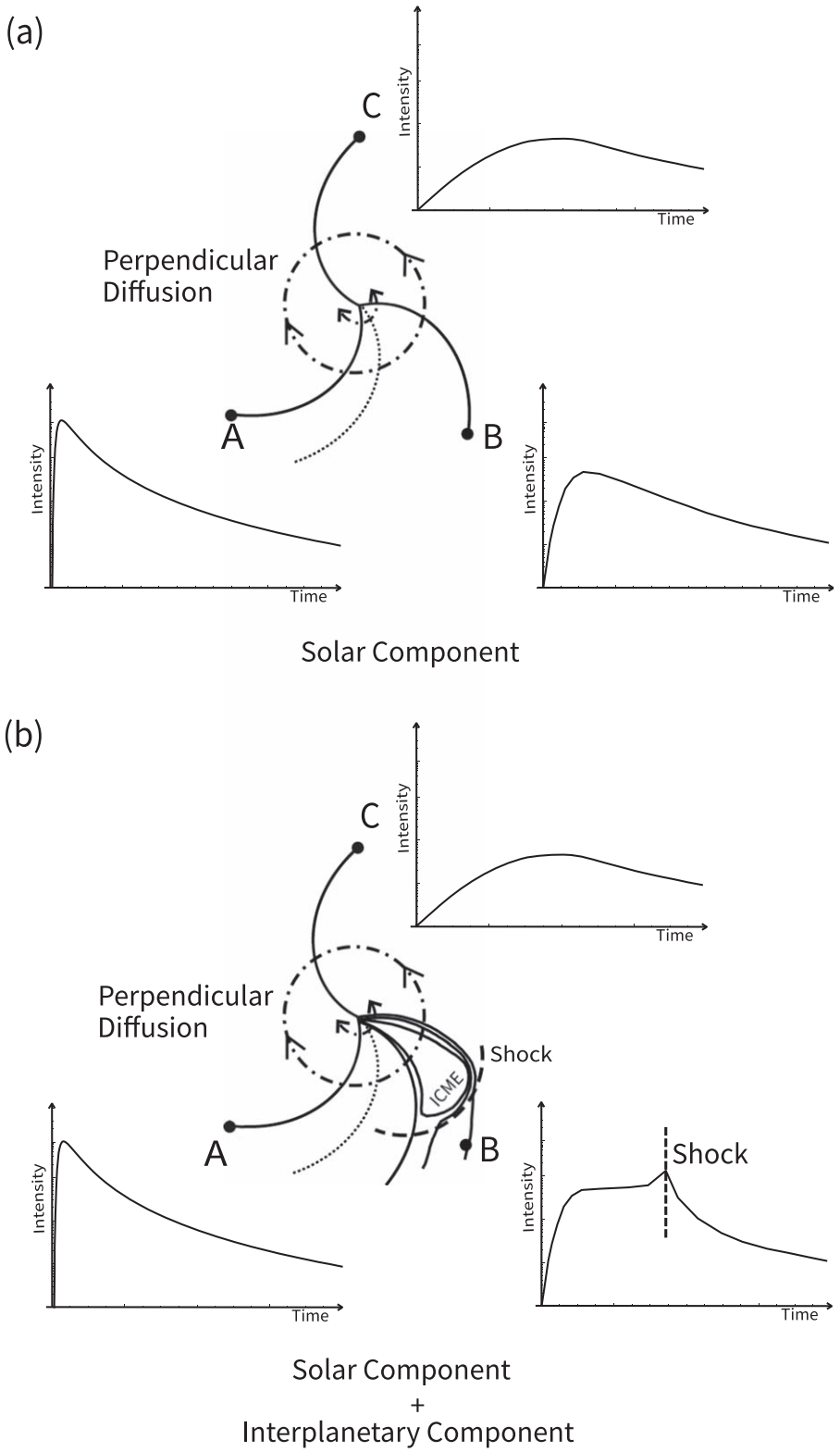

Figure 6. Panels (a) and (b) represent the diffusion of >10 MeV energetic protons in the absence and presence of the acceleration of interplanetary shock, respectively. The solid black lines represent the MFLs. Spacecraft A, B, and C are near 1 AU in the ecliptic. The dotted lines represent the magnetic field line connected to the strongest acceleration part of the solar source region. The inner and outer dotted dashed lines represent the effects of perpendicular diffusion of particles near the Sun and in interplanetary space, respectively.

affect the peak of the intensity observed by spacecraft A. Similar to spacecraft A shown in panel (a), the peak in particle intensity consists mainly of the solar component. Among the three spacecraft, the peak intensity observed by spacecraft A is the largest, so spacecraft A is the HPI spacecraft.

*Spacecraft B.*Unlike in panel (a), in panel (b) the solar component of coronal origin and the interplanetary component associated with interplanetary shocks are both important in the intensity–time profiles observed by spacecraft B. For an interplanetary shock driven by ICME, the strongest

acceleration is in the central part of the shock, near the nose of the shock (Cane et al. 1988). The nose of the shock in the diagram is pointing toward spacecraft B, so particles accelerated by the interplanetary shock can reach spacecraft B easily. In this case, two peaks of particle intensity may be observed by spacecraft B. The first peak is the solar component that undergoes perpendicular diffusion to reach spacecraft B, and the second peak is the interplanetary component produced by the acceleration of interplanetary shock. The relative magnitude of the two peaks depends on the strength of the solar source region, the distance of spacecraft B's magnetic footpoint from the solar source region, and the strength of the shock acceleration, etc. In most cases, the acceleration of >10 MeV protons in the solar source region is much stronger than in the acceleration by interplanetary shock. The contribution of the interplanetary component depends on the shock's strength of acceleration and the direction of the shock nose relative to the observer. On the other hand, the contribution of the solar component depends on the solar source strength and the distance between the solar source and the footpoint of the observer. If the contribution of the solar component is larger than that of the interplanetary component, the first peak could be larger than the second one. Otherwise, the second peak could be larger than the first one.

Spacecraft C. Unlike in panel (a), in panel (b) the particles observed by spacecraft C have both a solar component and an interplanetary component. Most of the particles undergo perpendicular diffusion to reach the MFLs of spacecraft C. Particle acceleration in the solar source region is much stronger than the acceleration by interplanetary shock, and the shock is far away from spacecraft C. Therefore, the solar component dominates the interplanetary component, and particles observed by spacecraft C are still mainly from the solar source, rather than the interplanetary shock.

4. Conclusions

In this work, we have analyzed the intensity–time profiles of 13–64 MeV energetic proton intensities observed by the STEREO A, STEREO B, and SOHO spacecraft from 2010 July to 2014 September. In gradual energetic proton events, we often find that the ratio of peak intensities observed at different locations in the same event remains almost constant as the energy varies. In other words, the ratio of peak intensities from the different energy channels remains almost constant as the position of the spacecraft changes. We call these relations equal ratio relations. It suggests that particles observed by the spacecraft at different locations originated from the same acceleration process. We find that in the cases without ESP events or multiple peaks, the peak times of intensities for >10 MeV energetic protons observed by the HPI spacecraft are often only a few hours to a dozen hours, or at most a day, after solar eruptions. Therefore, the acceleration of particles usually takes place in the vicinity of the Sun, rather than in interplanetary space.

According to the paradigm of Cane et al. (1988), the acceleration efficiency of the shock varies with longitude, with the strongest acceleration near the nose of the shock and weaker acceleration toward the flanks. If energetic particles are accelerated by interplanetary shocks, the properties of the event can be explained on the basis of the large-scale structure of the interplanetary shocks. Assuming that perpendicular diffusion can be neglected during interplanetary propagation, particles observed by the spacecraft depend mainly on the particle injection process and the parallel diffusion along the magnetic lines. In this case, the injection processes of particles are different at different locations in the interplanetary space. For the shock acceleration, the intensity–time profiles observed by spacecraft are sensitive to the shock acceleration strength at the intersection of the field line on the shock. If the paradigm of Cane et al. (1988) were true, there would be no equal ratio relations between the peak intensities of particles observed by multiple spacecraft at different locations.

Contrary to the paradigm of Cane et al. (1988), for >10 MeV protons, we propose that the observations do not support that interplanetary shocks have a decisive effect on the longitudinal distribution of intensity–time profiles of energetic protons. For >10 MeV energetic protons, the perpendicular diffusion process could play a key role in the longitudinal distribution of gradual solar energetic protons, while the acceleration of interplanetary shock is less important. No matter if the acceleration by interplanetary shocks is strong or not, the effects of perpendicular diffusion can make multiple spacecraft at different longitudes observe energetic particle events, provided that there are enough particles accelerated near the Sun.

Without the acceleration by interplanetary shocks, the peak intensities of energetic particles observed multiple spacecraft at different longitudes often satisfy the equal ratio relations. Energetic particles observed at different locations consist mainly of solar components that undergo perpendicular diffusion in both the vicinity of the Sun and interplanetary space. Therefore, we propose an explanation that in gradual energetic proton events satisfying equal ratio relations, energetic particles in space are mainly composed of solar components, and perpendicular diffusion is the main factor that makes energetic particles observable in regions disconnected from the solar source by MFLs, with interplanetary shocks not playing a dominant role in the process. Previous studies of the reservoir phenomenon suggest that perpendicular diffusion plays an important role in the decay phase of particle intensities (McKibben et al. 2001a, 2001b; Zhang et al. 2009; Lario 2010; Qin et al. 2013; Qin & Wang 2015). In this work, we suggest that the effects of perpendicular diffusion are important for the transport of energetic particles not only during the decay phase but also throughout the rising phase. For >10 MeV protons, in many events intensity–time profiles can be understood as a result of perpendicular diffusion rather than that as a consequence of acceleration by the interplanetary shocks.

Among many of the SEP events studied in our work, there are only a few events with significant acceleration of >10 MeV energetic protons by interplanetary shocks. Interplanetary shocks mainly affect the observations of spacecraft in the direction of the strongest acceleration (along the direction of the shock nose), and two peaks of particle intensity can be observed by spacecraft. In most cases, the acceleration of the solar source is much stronger than the acceleration by the interplanetary shock. The impact of the interplanetary component relies on the shock's acceleration intensity and the orientation of the shock nose in relation to the observer. Conversely, the solar component's influence is determined by the strength of the solar source and the distance between it and the observer's footpoint. In cases where the solar component's contribution surpasses that of the interplanetary component, the first peak may exceed the second. Alternatively, if the interplanetary component's contribution is greater, the second

peak could be more prominent than the first. If particles accelerated by an interplanetary shock form an ESP event, there is both a solar component in interplanetary space originating from the solar corona and an interplanetary component originating from the interplanetary shock. The mixing of two different components does not result in equal ratio relations in the peak intensities observed by spacecraft at different locations.

In conclusion, the varying observations of energetic solar proton events could be explained if they are organized according to the longitude of the source and considering the effects of perpendicular diffusion. The onset times observed by spacecraft at different locations, the equal ratio relations of the peak intensities, and the reservoir phenomena in the decay phase, could all be explained by the effects of perpendicular diffusion. For >10 MeV protons, generally, most interplanetary shocks do not significantly accelerate protons or produce ESP events. In this case, the solar component dominates, and perpendicular diffusion is responsible for the large-scale longitudinal distribution of energetic particles. In a few events, the interplanetary component is important if ESP events are present. However, the efficient acceleration of interplanetary shock is mainly in the direction of the shock nose, with a quick decay of the acceleration efficiency toward the flanks, so perpendicular diffusion is responsible for the large-scale longitudinal distribution of energetic particles. In our previous studies, some of the results in this work have been obtained with numerical simulations (Zhang et al. 2009; Wang et al. 2012; Qin et al. 2013; Qin & Wang 2015). In the future, we will further study this problem with both observations and simulations.

Acknowledgments

The authors thank the anonymous referee for their valuable comments. We are partly supported by grants NNSFC 41774182, NNSFC 42074206, NNSFC 41874206, Guangdong Basic and Applied Basic Research Foundation (No. 2023A1515011626), Shenzhen Key Laboratory Launching Project (No. ZDSYS20210702140800001), and Shenzhen Science and Technology Program under Grant No. JCYJ20210324132812029. We would like to acknowledge and express our gratitude for the energetic particle and plasma data provided by STEREO and SOHO. We also thank the CDA, OMNI, and NOAA for maintaining the spacecraft data online. This paper uses data from the Heliospheric Shock Database, generated and maintained at the University of Helsinki.

ORCID iDs

Yang Wang https://orcid.org/0000-0002-4581-9242
Gang Qin https://orcid.org/0000-0002-3437-3716

References

Bryant, D. A., Cline, T. L., Desai, U. D., & McDonald, F. B. 1962, JGR, 67, 4983
Cane, H. V., Reames, D. V., & von Rosenvinge, T. T. 1988, JGR, 93, 9555
Dalla, S., Marsh, M. S., Kelly, J., & Laitinen, T. 2013, JGRA, 118, 5979
Dresing, N., Gómez-Herrero, R., Heber, B., et al. 2014, A&A, 567, A27
Dresing, N., Gómez-Herrero, R., Klassen, A., et al. 2012, SoPh, 281, 281
Gordon, B. E., Lee, M. A., Möbius, E., & Trattner, K. J. 1999, JGR, 104, 28263
He, H.-Q., Qin, G., & Zhang, M. 2011, ApJ, 734, 74
Heras, A. M., Sanahuja, B., Lario, D., et al. 1995, ApJ, 445, 497
Heras, A. M., Sanahuja, B., Smith, Z. K., Detman, T., & Dryer, M. 1992, ApJ, 391, 359
Jian, L. K., Russell, C. T., Luhmann, J. G., & Galvin, A. B. 2018, ApJ, 855, 114
Kallenrode, M. 2001, JGR, 106, 24989
Kallenrode, M., & Wibberenz, G. 1997, JGR, 102, 22311
Kilpua, E. K. J., Lumme, E., Andreeova, K., Isavnin, A., & Koskinen, H. E. J. 2015, JGRA, 120, 4112
Laitinen, T., & Dalla, S. 2017, ApJ, 834, 127
Laitinen, T., Dalla, S., & Marriott, D. 2017, MNRAS, 470, 3149
Lario, D. 2010, in AIP Conf. Proc. 1216, Twelfth Int. Solar Wind Conf., ed. M. Maksimovic et al. (Melville, NY: AIP), 625
Lario, D., Sanahuja, B., & Heras, A. M. 1998, ApJ, 509, 415
Lee, M. A. 1983, JGR, 88, 6109
Lee, M. A. 2005, ApJS, 158, 38
Li, G., Zank, G. P., & Rice, W. K. M. 2003, JGRA, 108, 1082
McKibben, R. B. 1972, JGR, 77, 3957
McKibben, R. B., Lopate, C., & Zhang, M. 2001a, SSRv, 97, 257
McKibben, R. B., et al. 2001b, ICRC (Hamburg), 3281
Ng, C. K., Reames, D. V., & Tylka, A. J. 1999, GeoRL, 26, 2145
Paassilta, M., Papaioannou, A., Dresing, N., et al. 2018, SoPh, 293, 70
Qin, G., & Wang, Y. 2015, ApJ, 809, 177
Qin, G., Wang, Y., Zhang, M., & Dalla, S. 2013, ApJ, 766, 74
Reames, D. V. 1999, SSRv, 90, 413
Reames, D. V. 2017, Solar Energetic Particles: A Modern Primer on Understanding Sources, Acceleration and Propagation, 932 (Berlin: Springer)
Rice, W. K. M., Zank, G. P., & Li, G. 2003, JGRA, 108, 1369
Richardson, I. G., et al. 2014, SoPh, 289, 3059
Roelof, E. C., Gold, R. E., Simnett, G. M., et al. 1992, GeoRL, 19, 1243
Rouillard, A. P., et al. 2011, ApJ, 735, 7
Sokolov, I. V., Roussev, I. I., Gombosi, T. I., et al. 2004, ApJL, 616, L171
Strauss, R. D., Dresing, N., Kollhoff, A., & Brüdern, M. 2020, ApJ, 897, 24
Strauss, R. D., le Roux, J. A., Engelbrecht, N. E., Ruffolo, D., & Dunzlaff, P. 2016, ApJ, 825, 43
Strauss, R. D. T., Dresing, N., & Engelbrecht, N. E. 2017, ApJ, 837, 43
van den Berg, J. P., Engelbrecht, N. E., Wijsen, N., & Strauss, R. D. 2021, ApJ, 922, 200
Verkhoglyadova, O. P., Li, G., Zank, G. P., Hu, Q., & Mewaldt, R. A. 2009, ApJ, 693, 894
Wang, Y., Lyu, D., Wu, X., & Qin, G. 2022, ApJ, 940, 67
Wang, Y., Lyu, D., Xiao, B., et al. 2021, ApJ, 909, 110
Wang, Y., Qin, G., & Zhang, M. 2012, ApJ, 752, 37
Wiedenbeck, M. E., Mason, G. M., Cohen, C. M. S., et al. 2013, ApJ, 762, 54
Wijsen, N., Aran, A., Sanahuja, B., Pomoell, J., & Poedts, S. 2020, A&A, 634, A82
Zank, G. P., Rice, W. K. M., & Wu, C. C. 2000, JGR, 105, 25079
Zhang, M., Qin, G., & Rassoul, H. 2009, ApJ, 692, 109
Zhang, M., & Zhao, L. 2017, ApJ, 846, 107